Available online at www.sciencedirect.com
ScienceDirect
Journal of Power Sources 178 (2008) 334–343
JOURNAL OF POWER SOURCES
www.elsevier.com/locate/jpowsour

Air plasma spray processing and electrochemical characterization of SOFC composite cathodes

B.D. White [a], O. Kesler [b,*], Lars Rose [c,d]

[a] *Department of Mechanical Engineering, The University of British Columbia, 2054-6250 Applied Sciences Lane, Vancouver, British Columbia, Canada V6T 1Z4*
[b] *Department of Mechanical and Industrial Engineering, University of Toronto, 5 King's College Road, Toronto, Ontario, Canada M5S 3G8*
[c] *Department of Materials Engineering, The University of British Columbia, 309-6350 Stores Road, Vancouver, British Columbia, Canada V6T 1Z4*
[d] *National Research Council Canada, Institute for Fuel Cell Innovation, 4250 Wesbrook Mall, Vancouver, British Columbia, Canada V6T 1W5*

Received 31 August 2007; received in revised form 17 November 2007; accepted 19 November 2007
Available online 26 November 2007

Abstract

Air plasma spraying has been used to produce porous composite cathodes containing $(La_{0.8}Sr_{0.2})_{0.98}MnO_{3-y}$ (LSM) and yttria-stabilized zirconia (YSZ) for use in solid oxide fuel cells (SOFCs). Preliminary investigations focused on determining the range of plasma conditions under which each of the individual materials could be successfully deposited. A range of conditions was thereby determined that was suitable for the deposition of a composite cathode from pre-mixed LSM and YSZ powders. A number of composite cathodes were produced using different combinations of parameter values within the identified range according to a Uniform Design experimental grid. Coatings were then characterized for composition and microstructure using EDX and SEM. As a result of these tests, combinations of input parameter values were identified that are best suited to the production of coatings with microstructures appropriate for use in SOFC composite cathodes. A selection of coatings representative of the types of observed microstructures were then subjected to electrochemical testing to evaluate the performance of these cathodes. From these tests, it was found that, in general, the coatings that appeared to have the most suitable microstructures also had the highest electrochemical performances, provided that the deposition efficiency of both phases was sufficiently high.

Keywords: SOFC; Plasma spraying; Composite cathode; LSM; YSZ

1. Introduction

Solid oxide fuel cells (SOFCs) are electrochemical energy conversion devices that could potentially provide low pollution, high efficiency energy for many power generation applications. SOFCs have the ability to make use of a wide variety of fuels including hydrocarbons, alcohols, hydrogen, and carbon monoxide, allowing them to provide a potential bridge between the existing fossil fuel economy and a future energy system incorporating hydrogen and/or renewable biomass fuels. The high temperature waste heat that they produce is suitable for cogeneration, making SOFC technology well suited for medium to large-scale stationary power generation applications and dramatically improving overall system efficiency [1].

While SOFC technology has significant potential, there are many substantial barriers preventing its widespread adoption at present. One concern stems from the difficulty and cost of scaling up existing manufacturing techniques for mass production. Wet ceramic processing techniques such as extrusion, tape casting, screen-printing, and spin coating are by far the most common processing techniques currently employed for SOFC fabrication [2]. These techniques generally require multiple fabrication steps for each of the cell layers (anode, cathode, electrolyte, and interconnects), interspersed by high temperature sintering or co-sintering steps. This is necessitated due to each layer generally

* Corresponding author. Tel.: +1 416 978 3835; fax: +1 416 978 7753.
E-mail addresses: bdwhite@interchange.ubc.ca (B.D. White), kesler@mie.utoronto.ca (O. Kesler), lars.rose@nrc-cnrc.gc.ca (L. Rose).

0378-7753/$ – see front matter © 2007 Elsevier B.V. All rights reserved.
doi:10.1016/j.jpowsour.2007.11.061

having different heating requirements to avoid over or under sintering or undesired reactions that create inactive or detrimental phases [3]. Thus, to achieve the high rates of production required to serve a large commercial market would require a large investment in equipment to create multiple, parallel production lines.

There is also a drive to reduce the cost of SOFCs by supporting the cell on metallic cell interconnects rather than using expensive rare-earth ceramics, such as $LaCrO_3$, that are traditionally used as interconnect materials for high temperature SOFCs, or anode supports, which use thicker layers of more expensive material [4]. Supporting the cells mechanically on the cheaper metallic interconnects allows the use of thinner layers of the more expensive anode, cathode, and electrolyte layers. This decreased thickness of active layers both lowers the cost of the cells and increases performance by reducing barriers to diffusion and conductivity. By replacing these interconnect ceramics and anode support layers with relatively inexpensive metals such as nickel or stainless steel, the cost of SOFCs can be significantly lowered. Additionally, metal interconnects offer improved thermal and electronic conductivity and ease of fabrication compared to ceramic interconnects [5]. Metal interconnects are also more robust and can be more rapidly thermally cycled to the cell operating temperature.

The use of metals, however, imposes significant constraints on both processing and operating temperatures, typically requiring expensive inert atmosphere furnaces for cell fabrication combined with lower electrolyte sintering temperatures, which can make densification more challenging. Densification also often involves the addition of sintering aids to the electrolyte, which can have detrimental effects on the ionic conductivity. Operating temperatures are also limited to below ~800 °C for coated interconnects. Unfortunately, the lower operating temperatures required by these materials significantly lowers the performance of SOFCs, thus creating the need for highly optimized electrode microstructures and thin electrolytes to achieve sufficiently high power densities [4,6–9].

Due to significant losses caused by relatively slow kinetics and low electronic conductivity, particularly in reduced temperature operation, SOFC cathodes are the subjects of much research [10]. Electrochemical activity in an SOFC cathode occurs at triple phase boundaries (TPBs), where gaseous oxygen and ionic and electronic conducting phases come into contact. The material most commonly used in SOFC cathodes, particularly in tubular cells, is $La_{1-x}Sr_xMnO_{3-y}$ (LSM), a perovskite that acts both as a catalyst as well as the electronic conductor. The electrolyte material, typically 8 mol% yttria-stabilized zirconia (YSZ) [11], provides ionic conductivity and additional catalytic activity when combined with the LSM in a cathode composite. The greater the length of the triple phase boundaries, the greater the cathode activity and the better the cell performance is. Thus, one strategy for improving cathode performance is to increase the length of TPBs by using a composite cathode structure, containing both LSM and YSZ. TPBs are thereby extended beyond the cathode/electrolyte interface, into the cathode bulk, thus greatly enhancing cathode activity and performance [12]. Porosity also affects cathode performance, particularly when operating at high current densities at which the diffusion of O_2 to reaction sites becomes the rate limiting process. Porosity levels in composite cathodes of 30–40% are often found to be desirable to avoid detrimental reactant mass transport effects [13,14].

Plasma spray processing has traditionally been used to deposit ceramic coatings for wear resistant and thermal barrier applications. Increasingly, many SOFC researchers regard plasma spray processing as having the potential to overcome the limitations of conventional manufacturing processes [15–17]. Plasma spraying uses an electric arc to heat and ionize gases, typically argon, helium, hydrogen, and nitrogen, to produce an energetic plasma. The gasses are fed into the torch in varying amounts depending on the desired properties of the plasma. Particles of the material to be sprayed are fed into the hot plasma; they absorb heat and are accelerated towards the substrate at speeds of approximately $500\,m\,s^{-1}$. The two principal variations of plasma spraying atmospheres are air plasma spraying and vacuum plasma spraying, where air and vacuum refer to the conditions under which the process is carried out. Air (or atmospheric) plasma spraying (APS) involves spraying in air at atmospheric pressure, while vacuum plasma spraying (VPS) is carried out in an evacuated chamber (typically ~0.1 atm).

Plasma spraying has the advantage of high speed of processing that can be achieved by reducing or eliminating the need for sintering, thus allowing the cell layers to be deposited in rapid succession. By eliminating high temperature sintering of the cell layers, the use of metal interconnects is also greatly simplified. The entire SOFC can be deposited onto a relatively cool metal interconnect substrate without the risk of oxidation of the metal. In addition to allowing for continuous deposition, the plasma spraying process is easily automated, thus making the process particularly well suited for mass production. Plasma spraying can also potentially be used to achieve greater control over the spatial variation of the microstructure and composition of the cell layers and for the creation of functionally graded cell components [17,18].

There are a number of plasma spray input parameters that are generally acknowledged to have a significant effect on the quality of coatings produced. Some of the more important input parameters include electrode current, plasma gas flow rate, plasma gas composition, powder carrier gas flow rate, powder feed rate, powder particle size, standoff distance (SOD), and substrate temperature [19]. By varying the value of these parameters, substantial differences in coating strength, adhesion, and porosity can be realized.

The majority of research conducted thus far has focussed on the use of vacuum plasma spraying (VPS) in the manufacture of cathodes, both single phase and composite. It has been demonstrated that SOFCs fabricated by VPS can achieve performance levels similar to those fabricated by traditional techniques [18,20]. More recently, there have been attempts to fabricate SOFCs using atmospheric plasma spraying (APS), taking advantage of the relative simplicity and lower cost of the process [21]. While this work has shown that APS is suitable for the fabrication of well performing SOFCs, APS cathode work thus far has been largely confined to single phase cathodes. Through the use of composite cathodes it could be expected that the performance of APS SOFCs could be significantly increased.

In the present paper, work leading to the development of an LSM/YSZ composite cathode produced by APS is presented. Preliminary work examined the preparation and deposition of the two materials, LSM and YSZ, individually in a series of screening trials designed to determine the appropriate range of plasma conditions for each material. Following these screening trials, composite coatings were produced using the previously determined ranges for the plasma conditions. Following characterization of these coatings for microstructure and composition, electrochemical impedance spectroscopy (EIS) was used to evaluate their performance.

2. Experimental procedure

2.1. Material preparation

In this work, LSM feedstock powder with composition $(La_{0.8}Sr_{0.2})_{0.98}MnO_{3-y}$ (Infrox^{TM} S5725SR, Inframat Advanced Materials, Farmington, CT, U.S.A.) was used. The LSM powder was spray dried, producing spherical agglomerates. The as-received powder had a d_{50} agglomerate size (on a volume basis) of approximately 47 μm, with sizes ranging from 10 μm to 100 μm, as determined by laser light scattering particle size analysis (Mastersizer 2000, Malvern Instruments, Worcestershire, U.K.). In order to prevent the break up of the spray dried LSM agglomerates during feeding, which was found to clog the powder feed lines, the as-received powder was heated for 6 h at 1175 °C. This calcining step was found to provide better cohesion of the spray dried agglomerates, and prevented further clogging of the feed lines. The calcined powder was then sieved into narrower size fractions, resulting in usable size distributions of −75 + 45 μm and −45 + 32 μm.

The YSZ powder used for the initial screening tests contained 4.7 mol% Y_2O_3 (920410-75MIC, St. Gobain, Worcester, MA, U.S.A.) due to its low cost. This composition is typical for Thermal Barrier Coating quality YSZ, but has a significantly lower Y_2O_3 content than the 8–10 mol% normally used in SOFC applications. While the electrical performance of this YSZ powder is expected to be poor due to slightly lower intrinsic ionic conductivity and the presence of impurities, the physical properties of the powder are expected to be similar to those of electrical quality YSZ, thus making the powder suitable for initial screening tests. The as-received YSZ powder had a size distribution from 10 μm to 124 μm with a d_{50} of approximately 50 μm. The powder was sieved into narrower size distributions of −75 + 45 μm, −45 + 32 μm, and −32 + 10 μm.

For spraying experiments following the initial screening tests, high purity, electrical quality, spray dried 8 mol% YSZ (8YSZ) was used (Nanox S408A, Inframat Advanced Materials, Farmington, Connecticut, U.S.A.). This powder had a size distribution in the same range as that of the LSM. Heat treatment was again required to prevent break-up of the agglomerates, at 1350 °C for 5.5 h. The 8YSZ powders were sieved to size ranges of −45 + 32 μm and −32 + 25 μm.

For deposition of composite cathodes, the LSM and YSZ powders were dry mixed and fed from one hopper (Thermico, model CPF-2HP, Germany). This approach was taken as previous work involving the co-deposition of LSM and YSZ from separate hoppers has indicated that the resulting coating can consist of alternating layers of the two materials, rather than uniform percolation of both phases [20].

For the plasma sprayed electrolytes used in the symmetric cathode cells for electrochemical testing, fine (−25 μm), calcined 8 mol% YSZ powder was used.

2.2. Plasma spray processing and coating characterization

The APS system used in these experiments (Axial III Series 600, Northwest Mettech Corp., North Vancouver, BC, Canada) contains three cathodes and uses axial powder injection. Axial powder injection ensures that virtually all of the powder injected passes through the hottest part of the plasma jet, thus facilitating the uniform melting of the powder. Deposition was carried out onto sandblasted stainless steel substrates mounted on a turntable rotating at 400 rpm. The rotation of the substrates provided cooling during the deposition process.

Preliminary screening tests were carried out with both LSM and YSZ separately in order to determine the range of parameter values over which each material could be successfully deposited. The parameters considered were torch current, plasma gas composition, plasma gas flow rate, and standoff distance. All of the coatings produced for the screening tests were deposited onto sandblasted stainless steel coupons.

With LSM coatings, the primary concern was ensuring that there was minimal decomposition of the LSM phase. X-ray diffraction (XRD) analysis of the coatings was used to determine if decomposition of the LSM had occurred. Comparison of the relative intensity of the diffraction pattern peaks of the LSM and the decomposition products (e.g. La_2O_3) offered some indication of the extent of the decomposition. The LSM coatings were also checked for mechanical adhesion through the use of a simple scratch test. The LSM coatings tended to either be very easily removed, or well adhered to the substrate.

YSZ coatings presented a significantly different set of challenges than those encountered in the production of LSM coatings, largely centred on finding conditions to sufficiently melt the YSZ while not decomposing the LSM. YSZ is considerably more stable than LSM and does not decompose under most spraying conditions. YSZ coatings were therefore evaluated only for their adhesion to the substrates.

Following the identification of the usable range of parameter values, composite coatings were produced using a variety of parameter values within these ranges, and their suitability for use as cathodes was evaluated. In order to examine the effect of varying the above plasma spray input parameters on the composition and microstructure of the composite coatings, an experimental grid was developed to explore multiple combinations of parameter values within the ranges identified in the preliminary screening trials. The experimental grid developed used the Uniform Design technique, in which the combinations of parameter values are uniformly distributed over the experimental space. Four levels for each parameter were explored in 40 trials.

The coatings produced were examined by SEM and their composition evaluated by energy dispersive X-ray spectroscopy

(EDX). Reliable, quantitative total porosity measurements could not be obtained from these very thin coatings on porous substrates; the total coating porosity was therefore judged qualitatively from micrographs to obtain comparative porosity information for the different conditions as a screening step to identify coatings suitable for further characterization and electrochemical testing.

Mercury porosimetry (Micromeritics Autopore IV Mercury Porosimeter, Norcross, GA, U.S.A.) was performed on bare substrates and on cathode-coated substrates to identify the pore size distribution of the cathodes in comparison to that of the substrates for the cathodes having the best electrochemical performance. The porosimetry measurements were made in combination with XRD (Bruker AXS, Karlsruhe, Germany) theoretical density measurements and BET surface area analysis (Beckman Coulter SA3100, Fullerton, CA, U.S.A.) to produce calculations of the pore size distributions of each specimen.

Helium permeation experiments were also performed to determine the gas permeability of the best cathodes. These measurements were performed in a sealed jig designed in-house. The supplied helium gas was regulated by a pressure controller (Alicat Scientific, Model PCD-5PSIG-D, 2 pneumatic valves, Tucson, AZ, U.S.A.) to a set pressure at the inlet to the measurement chamber. After pressure stabilization, the flow of gas through the sample was measured at the outlet of the jig by a mass flow meter (Alicat Scientific, Model M-20SLPM-D_H2, Tucson, AZ, U.S.A). From the results of these assessments, observations about the effect of variations in some of the key processing parameters can be made.

2.3. Electrochemical testing

To compare the electrochemical performance of APS composite cathodes produced using different deposition conditions, a series of coatings from the Uniform Design study having representative microstructures were reproduced. For the electrochemical evaluation of the APS composite cathodes, cathode–cathode symmetric cells were deposited, along with plasma sprayed 8 mol% YSZ electrolytes, onto porous, 25.36 mm diameter, AISI 430 stainless steel substrates (Mott Corporation, Farmington, Connecticut, U.S.A.). Identical deposition conditions were used for the electrolyte in each cell. The deposition parameters used for these cathodes is given in Table 1. The ratio of LSM:YSZ in the starting powder mixture for the cathodes of the four cells was adjusted to yield final coatings having approximately the same proportion of the two materials by volume. The cathode–cathode symmetric cells produced for electrochemical testing had a desired thickness for each cathode of ~50 μm, while the desired thickness of the electrolyte was 20 μm. To achieve high density in the electrolyte layer, deposition was carried out in a high energy plasma (87 kW) using 100% N_2 with 250 A/cathode torch current at a standoff distance of 120 mm. As cells were being tested in a symmetric cell configuration, gas permeability of the electrolyte was not a major concern. The electrolyte needed only be sufficiently dense to allow for reasonably good ionic conductivity.

Electrochemical testing was carried out using a 25.4 mm cell diameter test stand with EIS measurements (SI 1260 frequency response analyzer, Solartron Analytical, Farnborough, U.K.) to determine the electrodes' polarization resistance and activation energy. Tests were performed at four temperatures between 750 °C and 900 °C in an air atmosphere with a total air flow rate to both sides of the symmetric cells of 0.1 slpm. Impedance measurements were carried out at OCV with an AC voltage amplitude of 20 mV over a range of frequencies between 1 MHz and 1–0.01 Hz, depending on the measurement temperature.

3. Results and discussion

3.1. Screening tests

Initial tests showed that the use of hydrogen as a plasma gas led to extensive decomposition of the LSM. Increasing the proportion of hydrogen in the plasma led to an increase in the extent of decomposition. In coatings produced using very energetic plasmas containing a high percentage of hydrogen combined with nitrogen, complete decomposition of the LSM occurred, resulting in mainly La_2O_3, as seen in Fig. 1a. The presence of even a small amount of hydrogen in the plasma, ~5 vol.%, was found to cause an unacceptable level of decomposition, as seen in Fig. 1b. When deposition was carried out in only argon/nitrogen plasmas, the extent of decomposition was greatly reduced or eliminated, as seen in the XRD pattern in Fig. 1c. The decomposition is likely the result of reduction of the LSM in the plasma, as it seems to be primarily the result of the presence of hydrogen rather than thermal effects, as determined by depositions performed at similar torch power levels both with and without hydrogen. Using argon/nitrogen plasmas, it was found that good LSM coatings could be obtained over a wide range of conditions, due in part to its relatively low melting temperature of 1880 °C.

Table 1
Plasma spray parameters used for deposition of cathode layers in the four symmetric cells prepared for electrochemical testing

	EC Cell 1	EC Cell 2	EC Cell 3	EC Cell 4
Standoff distance (mm)	100	100	100	180
Plasma gas flow rate (slpm)	217	250	183	250
Plasma composition	70% Ar, 30% N_2	23% Ar, 77% N_2	23% Ar, 77% N_2	46.7% Ar, 53.3% N_2
Carrier gas flow rate (slpm)	5	11.7	18.3	18.3
Arc current (A)	217	183	217	250
Powder size (LSM/YSZ)	−45 + 32 μm/−32 + 25 μm	−45 + 32 μm/−45 + 32 μm	−75 + 45 μm/−45 + 32 μm	−75 + 45 μm/−32 + 25 μm
Feed rate (g/min)	10	40	40	20
Nozzle diameter (mm)	12.7	9.52	12.7	12.7

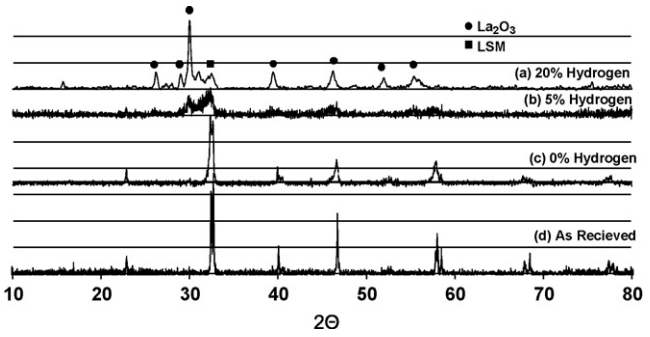

Fig. 1. XRD patterns of plasma sprayed LSM coatings produced with (a) 0% Ar, 80% N_2, 20% H_2; (b) 55% Ar, 40% N_2, 5% H_2; (c) 20% Ar, 80% N_2; and of (d) as-received LSM powder.

Coatings produced with $-75+45$ μm powder appeared to be more porous than those produced using the $-45+32$ μm LSM powder in less energetic plasmas, most likely due to the presence of partially melted particles in the coating.

Due to the need to co-deposit LSM and YSZ simultaneously in later stages of the project, it was necessary to produce YSZ coatings without the use of hydrogen as a plasma gas. The absence of hydrogen made it much more difficult to achieve conditions that would produce a good coating, as YSZ powder requires very energetic plasmas to melt due to its high melting point (2680 °C). Acceptable YSZ coatings were generally produced if the deposition conditions were such that at least some of the feedstock reached the substrate in a molten or partially molten state. Coatings were only successfully produced with the two smallest powder size ranges available, $-32+10$ μm and $-45+32$ μm. The argon/nitrogen plasma used was not sufficiently energetic to melt larger particles above 45 μm in diameter for most of the range of conditions explored.

From these preliminary screening tests it was determined that both LSM and YSZ could be deposited over a fairly wide range of overlapping conditions, presented in Table 2. LSM was fairly easy to deposit due to its relatively low melting point. Problems only occurred in very energetic plasmas, those with torch power greater than approximately 85 kW, where slight thermal decomposition of the LSM was noticed. The YSZ was more difficult to successfully deposit due to its higher melting point and the exclusion of hydrogen as a plasma gas. The $-32+10$ μm YSZ required a plasma power of at least 50 kW to produce a coating at low standoff distances (<150 mm). The deposition requirements of the LSM and YSZ defined the upper and lower bounds, respectively, of the usable range of plasma energies.

Table 2
Plasma spray parameter values identified from initial screening tests as suitable for both YSZ and LSM deposition, and used in experimental grid

Parameter	Values
LSM powder size (μm)	$-75+45$, $-45+32$
YSZ powder size (μm)	$-45+32$, $-32+10$
Powder feed rate (g min^{-1})	10–40
Plasma gas flow rate (slpm)	150–250
Carrier gas flow rate (slpm)	5–25
Vol.% Nitrogen (balance Ar)	30–100
Torch current (A $electrode^{-1}$)	150–250
Nozzle size (mm)	9.52–14.29
Standoff distance (mm)	100–340

3.2. Composite cathode production

Of the 40 trials in the Uniform Design experimental grid, 26 produced viable coatings that could be analyzed. The remaining 14 trials were either not performed due to system limitations or did not produce coatings that were sufficiently well adhered to the substrate for further characterization and testing.

The main difficulty in producing LSM/YSZ composite cathodes by APS is achieving the desired composition, ~50/50 vol.%, in the final coating due to the difference in deposition efficiency between the two materials for a given set of conditions, as shown in Fig. 2. The high melting point YSZ has lower deposition efficiency than the LSM in all of the spraying conditions explored. The relative deposition efficiency of the YSZ compared to the LSM was found to fluctuate significantly with variations in the input parameters from a low of 7% to a high of 74%, with the majority of coatings having between 30 and 60% YSZ deposition efficiency relative to that of LSM. Using this information, the YSZ content of the starting powder mixtures was increased to produce final coatings with the desired compositions. From a process efficiency point of view, higher deposition efficiencies are more desirable, as the total amount of material required, and therefore material costs, would be lower. Conditions resulting in very low YSZ deposition efficiencies would require large amounts of YSZ in the initial powder mixture, most of which would not end up in the coating and would be wasted or would require recycling of the powder as part of the manufacturing process. The parameters which appear to have the most significant and direct influence on the coating composition are the standoff distance, plasma gas composition, and relative particle size. The gun current, plasma gas flow rate, carrier gas flow rate, powder feed rate, and nozzle diameter appear to be less important, though they may play a more substantial role if higher order interactions were to be considered.

Variations in standoff distance appear to principally affect the relative amount of YSZ present in the final coating, with

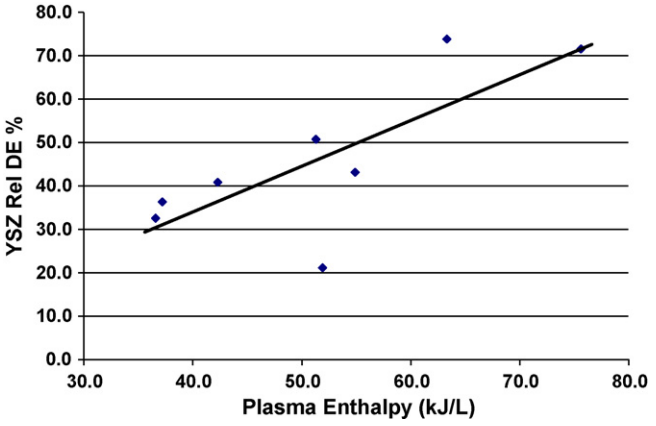

Fig. 2. Variation in YSZ relative deposition efficiency with total plasma enthalpy at 100 mm standoff distance.

coatings produced at small standoff distances containing significantly more YSZ. The deposition efficiency of the YSZ is much more sensitive to changes in standoff distance than that of the LSM. As previously mentioned, the presence of more YSZ in the final coating is desirable both for the extension of TPBs and because the incorporation of partially solid YSZ particles in the coating generates significant porosity. This effect can be seen in the micrographs in Fig. 3a and b. The coating produced at a shorter standoff distance contains a significantly higher percentage of YSZ, and appears to have a higher level of porosity. However, the LSM appears highly melted in both cases due to the high energy plasma used (>70 kW), resulting in a reduced internal cathode surface area and porosity.

The relative particle size of the LSM and YSZ can also affect the relative deposition efficiency by compensating for the large difference in melting temperature. By using large LSM particles and small YSZ particles, the relative deposition efficiency of the YSZ can be increased. However, the resulting powder mixture has a tendency to segregate into layers of each material during feeding, due to the vibration of the powder hopper. This segregation does not occur when using powders with more similarly sized particles. The microstructures of the coatings resulting from using powders with substantially different particle sizes also appear less uniform, with large LSM splats and finer YSZ structures, as seen in Fig. 4.

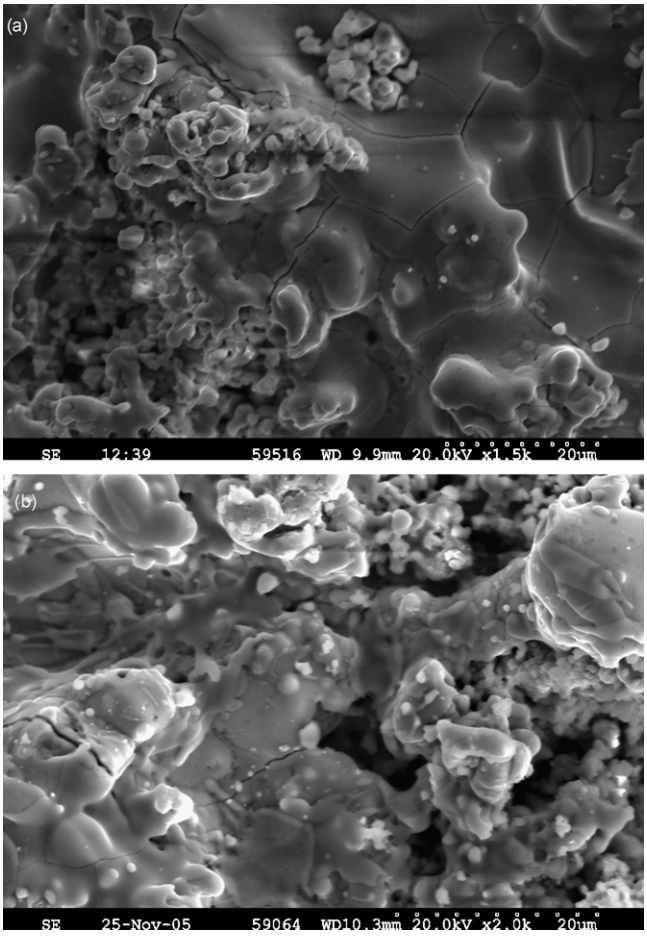

Fig. 3. SEM micrographs of LSM/YSZ APS coatings produced in high energy plasmas (>70 kW): (a) at 260 mm SOD, resulting in 15.5 vol.% YSZ and (b) at 100 mm SOD, resulting in 40.9 vol.% YSZ.

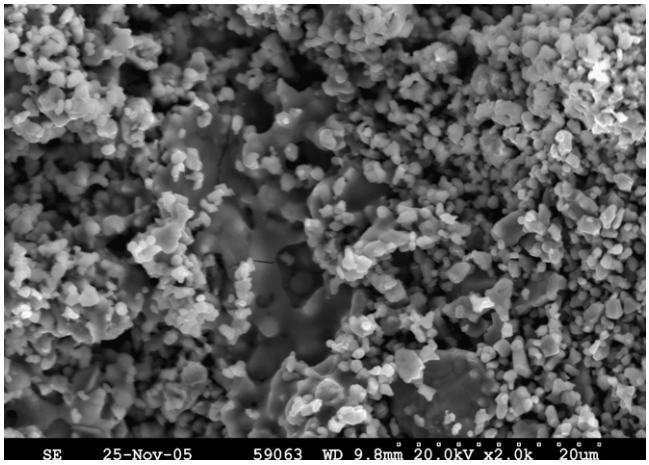

Fig. 4. SEM micrograph of LSM/YSZ APS coating produced using −75 + 45 μm LSM and −32 + 25 μm YSZ particles, showing segregation of fine YSZ particles from larger LSM splats.

Finally, the plasma gas composition also appears to play a significant role in determining the appearance of the coating microstructure and relative deposition efficiency of the YSZ. More energetic plasmas with higher nitrogen contents normally produce coatings with more YSZ, although this effect is sometimes overwhelmed by variations in other parameters. Increasing the plasma energy by increasing the torch current can have a similar effect, though the effect is much smaller than that observed by changing the plasma composition. The higher plasma energy also causes the LSM phase to melt more extensively, leading to a lower apparent coating porosity. Coatings produced using plasmas with lower energy density at short standoff distances, however, tend to have both LSM and YSZ remaining partially solid during deposition, generating significantly higher porosity levels in the coating, while still maintaining a significant amount of YSZ in the coating, as seen in Fig. 5. This combination of reasonable open porosity levels and reasonably high YSZ content is

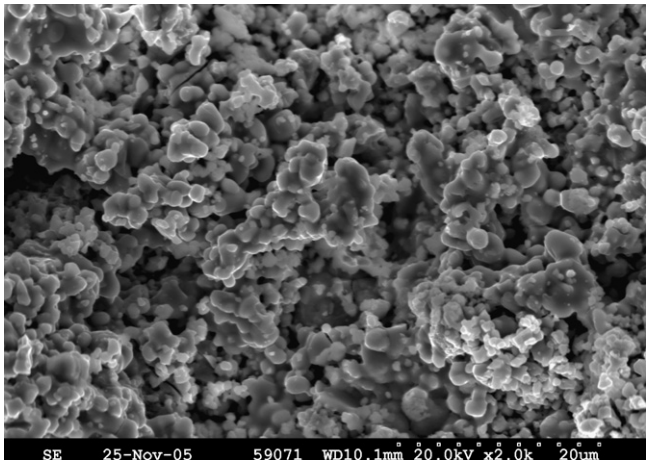

Fig. 5. SEM micrograph of LSM/YSZ APS coating produced in a lower energy plasma (50 kW) at 100 mm standoff distance, showing partially melted LSM, relatively high porosity, and 28.3 vol.% YSZ.

most desirable for SOFC cathodes. The low plasma energy density allows the LSM phase to remain somewhat porous, while the short standoff distance permits YSZ to reach the substrate while still in a partially molten state, without re-solidifying in-flight. The resulting coating has both composition and overall porosity in the range required to provide the high triple phase boundary lengths needed for a coating that is suitable for use as an SOFC composite cathode.

3.3. Symmetric cell electrochemical performance

For electrochemical testing, four sets of cathode deposition conditions were compared. These four cathodes were produced using a range of conditions to give microstructures ranging from partially melted and porous (EC Cells 1 and 2) to more dense and melted (EC Cells 3 and 4). SEM analysis of the surface of both cathodes in each cell revealed that their microstructures appeared to be very similar to those of the cathodes produced during the optimization study on sandblasted steel coupons. The microstructure of the two cathodes, one deposited directly on the metal interconnect and the other on top of the APS electrolyte, also appeared to be very similar. The surface views of the top cathodes can be seen in Figs. 6–9.

Due to large differences in the absolute deposition efficiency for the four cells, there were found to be significant differences in cathode thickness resulting from the spraying of similar amounts of material. This effect could, to some extent, be compensated for by changing the length of deposition time for cathode layers. This strategy was effective in EC Cells 2 and 3 in producing symmetric cells with similar layer thicknesses, as can be seen in Fig. 10. However, conditions used for deposition of EC Cells 1 and 4 have sufficiently low absolute deposition efficiency that reasonable increases in deposition time were not sufficient to produce a cathode layer with the desired thickness. Further, the cathodes deposited directly onto the metal substrate in these two cells appeared to be loosely enough adhered that they are partially removed during deposition of the electrolyte, resulting in a discontinuous cathode layer and a lowering of the active electrode area, as seen in Fig. 11.

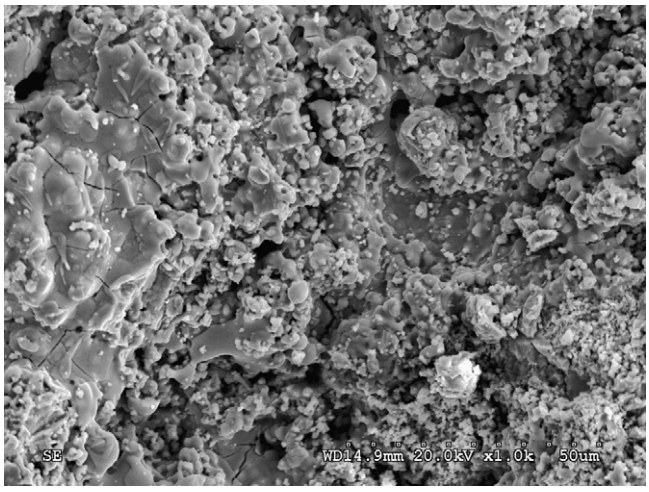

Fig. 7. Micrograph of top surface of EC Cell 2.

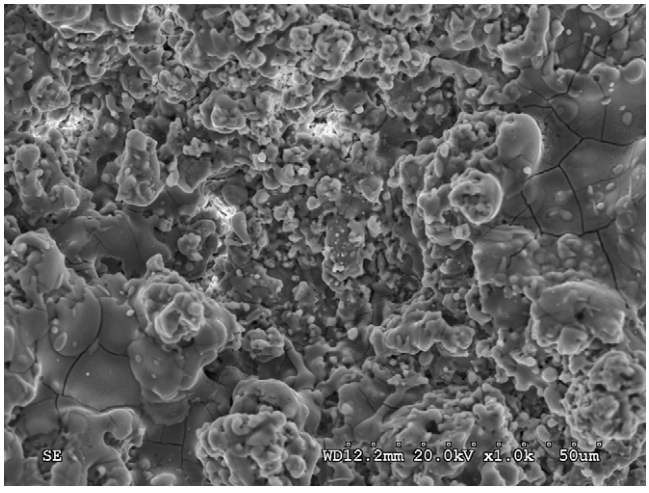

Fig. 8. Micrograph of top surface of EC Cell 3.

Nyquist plots for each cell at the various temperatures examined can be seen in Fig. 12. The corresponding Arrhenius plot of the cathode polarization resistances determined from the EIS testing of the four symmetric cells is shown in Fig. 13. As can

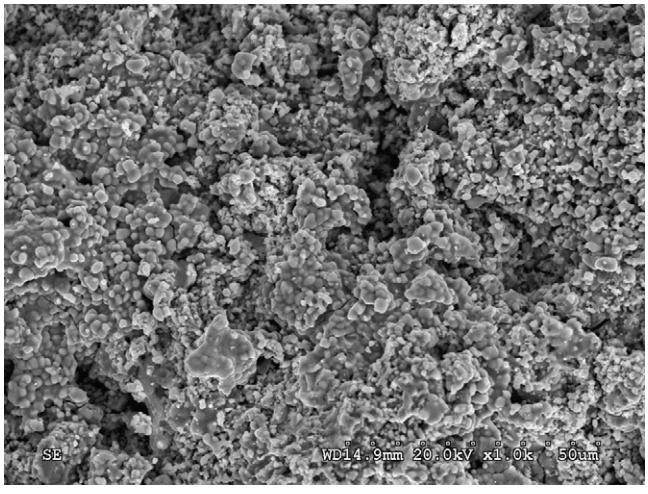

Fig. 6. Micrograph of top surface of EC Cell 1.

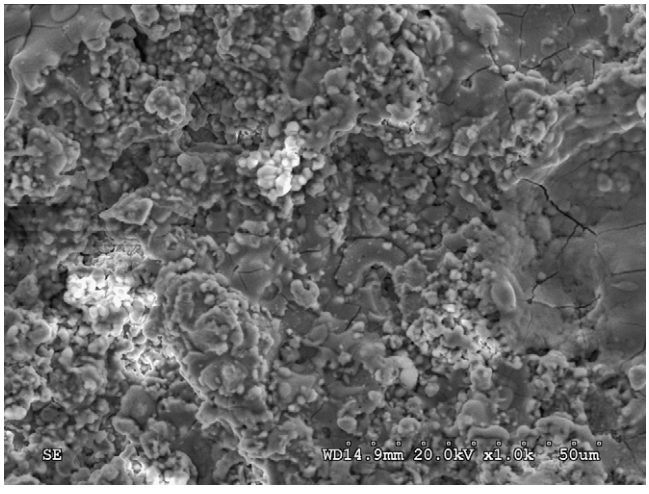

Fig. 9. Micrograph of top surface of EC Cell 4.

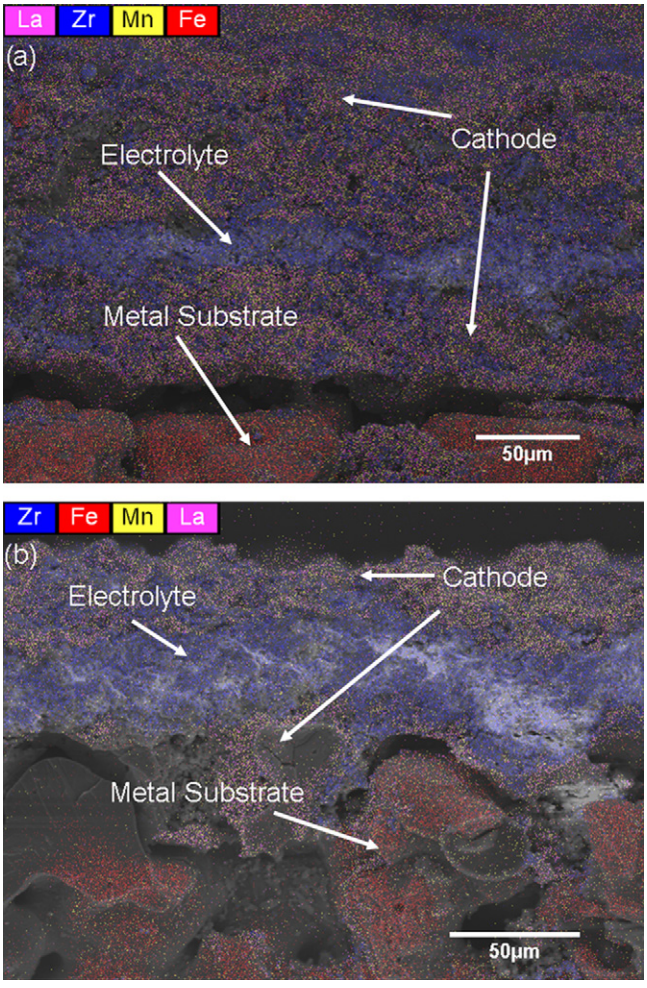

Fig. 10. Fracture cross section micrographs of symmetric cells EC Cell 2 (a) and EC Cell 3 (b).

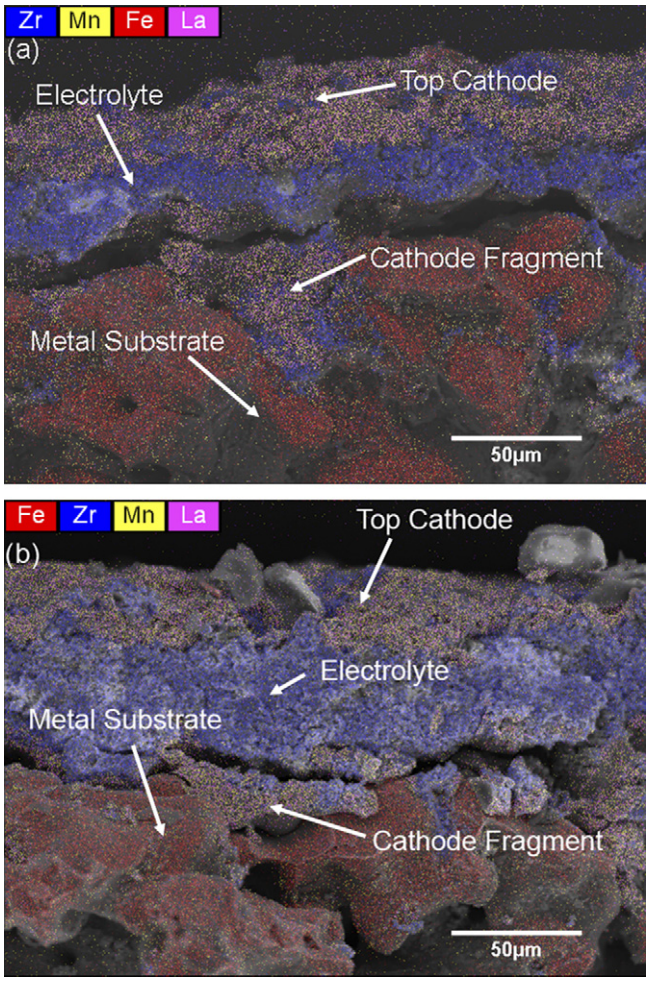

Fig. 11. Fracture cross-section micrographs of symmetric cells EC Cell 1 (a) and EC Cell 4 (b).

be seen from both the Nyquist and Arrhenius plots, EC Cell 2 had a polarization resistance significantly lower than that of the other three cells. Activation energy for all four cells was found to be between 0.95 eV and 1.47 eV, with the poorer performing cells having higher activation energies. EC Cell 1, which had initially appeared to have the most desirable microstructure, was in fact found to have the worst performance of the four cells. This can most likely be attributed to the reduction in active electrode area resulting from both poor adhesion to the substrate and low deposition efficiency leading to a less continuous (less fully formed) cathode layer, as discussed above. Similarly, EC Cell 4, which had a microstructure appearing less dense and melted than EC Cell 3, was found to have comparable polarization resistance. Again in this case, it is likely that the performance of this cell was reduced by the loss of active electrode area. When deposition conditions are such that both reasonable deposition efficiency and coating porosity can be obtained, as in EC Cell 2, the polarization resistance of cathodes produced by APS can be very low. Although it is possible that the relative composition of YSZ was also lower in the lower performing cells (1 and 4) than in the other EC cells due to differences in the relative deposition efficiencies of the YSZ and LSM, the initial starting powder mixtures were already adjusted to account for these differences to attain the same target compositions for each of the cells. Therefore, if a sufficient YSZ content still can not be achieved after that adjustment, then the deposition efficiency is in any event too low for those spraying conditions to make them viable for cathode coating production.

In EC Cell 2, the coating porosity was observed to be sufficiently high to allow a high triple phase boundary surface area to be produced, as seen from the low polarization resistance achieved by EC Cell 2 under open circuit conditions. At higher current densities, gas transport through the cathode becomes a more significant factor in the overall cell performance and needs to be considered in further optimization work to be performed on the cathode coatings.

Fig. 14 shows pore size distributions determined by mercury porosimetry on both uncoated porous metallic substrates and on substrates coated with one cathode layer of the cathode used in EC Cell 2. The results show that there are larger, approximately 14 μm on average, pores in the substrate, while the deposited cathode has a range of pore sizes not present or present in lower quantities in the bare substrates, with pore sizes ranging from approximately 0.4 to 12 μm. These results indicate that the cathode coating has porosity in a size range not

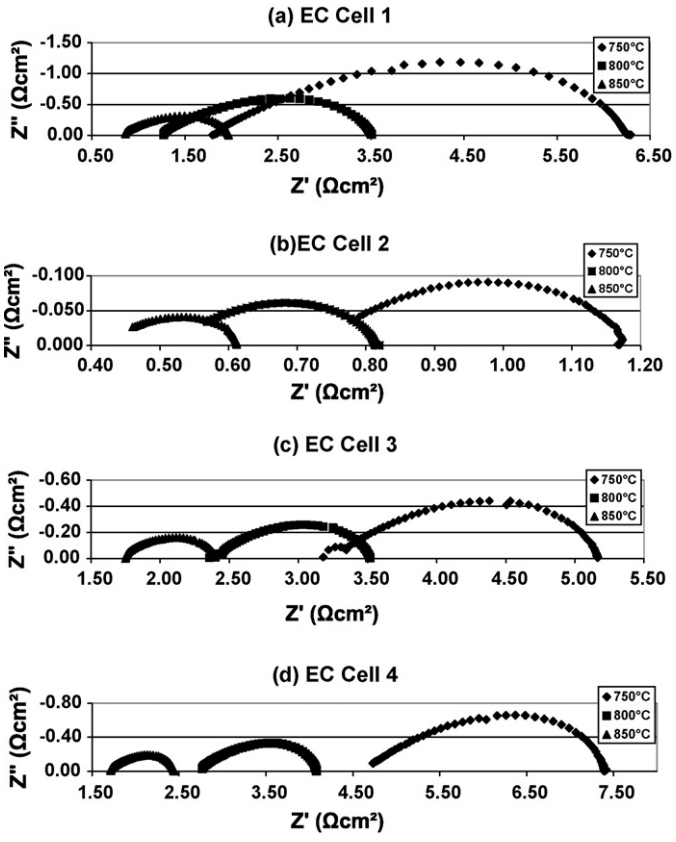

Fig. 12. Nyquist plots showing results of EIS for cells EC Cell 1 (a), EC Cell 2 (b), EC Cell 3 (c), and EC Cell 4 (d) at 750 °C, 800 °C, and 850 °C.

present in the substrate layers alone. However, due to the fairly thin and irregularly shaped cathode coating being supported on a much larger porous current collector support layer, the mercury porosimetry measurements of pore size distribution can not provide precise information about the total porosity of the cathode alone. In order to gain insight into whether the cathodes in EC Cell 2 would have sufficient porosity for use in high current density operating conditions, additional information is needed.

Ex situ helium gas permeation measurements were therefore performed on single cathode coatings of the type used in EC Cell

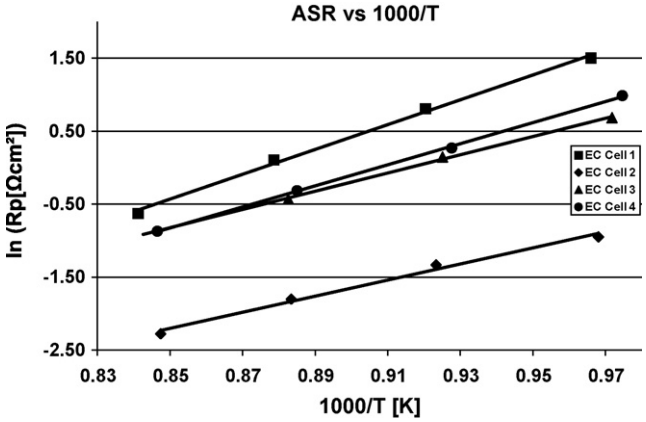

Fig. 13. Arrhenius plot showing polarization resistance and activation energy for the four cells.

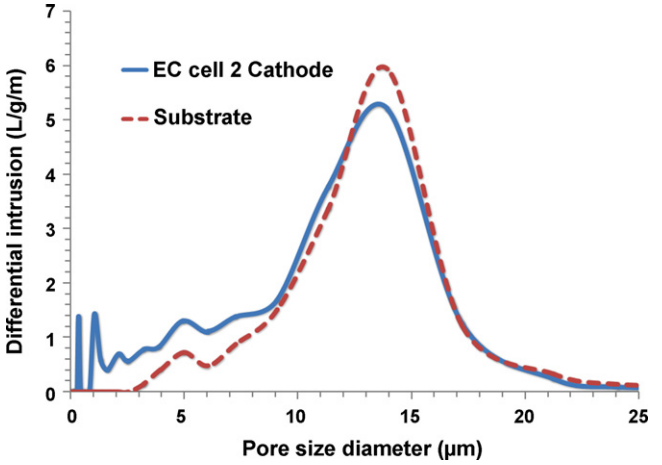

Fig. 14. Pore size distributions determined by mercury porosimetry for bare substrates and for substrates with one cathode layer sprayed with the same conditions as the cathodes in EC Cell 2. Each curve is the average curve of two specimens.

2 on the metal substrates, with the results shown in Fig. 15. The gas permeation results were limited by the cathodes, since permeation rates through the uncoated substrates (not shown here) were found to be approximately one order of magnitude higher than those through the cathode-coated substrates. The flow rate of helium gas through the cathode coating on a substrate was approximately 0.19 mL min^{-1} at 7 kPa gas pressure (a typical gas feed pressure in the laboratory electrochemical tests).

Although the flow rates of the smaller He gas molecules are likely somewhat larger than flow rates of air through the same cathode in the same conditions, the permeation tests can nevertheless provide some insight into whether the porosity in the cathodes is sufficient at higher current density operating conditions. For air flow rates comparable to the gas permeation rates measured in the ex situ tests at a similar gage pressure, a current density slightly higher than 3 A cm^{-2} could theoretically be supported by that air flow rate at typical fuel cell operating conditions of 25% oxidant utilization. That current density corresponds to a power density of over 2 W cm^{-2} at 0.7 V under

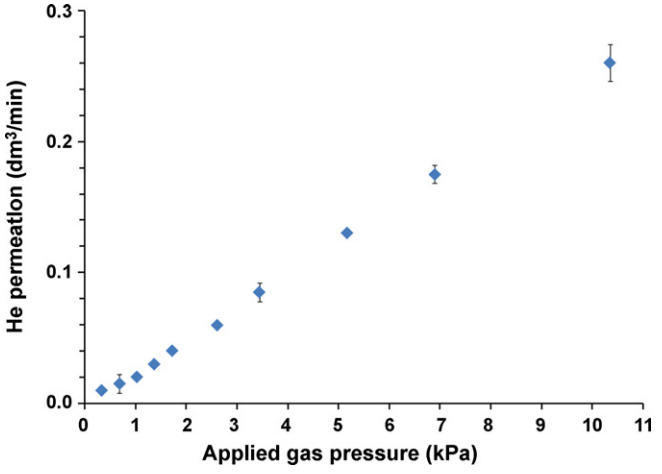

Fig. 15. Helium gas permeation through a substrate with a cathode coating sprayed with the same conditions as the cathodes in EC Cell 2.

those conditions. This result suggests that if a fuel cell with the deposited cathode would operate in a current density range lower than approximately 3 A cm^{-2}, its performance would likely be kinetics-limited, with gas diffusion limitations only appearing at substantially higher current densities. Thus, the porosity in the EC Cell 2 cathode should be sufficient for low to moderately high current density operation, while for a high-performing fuel cell operating at very high current densities, mass transport limitations would likely become rate-limiting.

In a planar cell with bi-polar plate interconnects, the fuel and oxidant would be fed in directions parallel to the plane of the cell, thus increasing the relative importance of diffusion perpendicular to the gas flow for supplying reactants to the cell rather than the perpendicular gas flow utilized in both the button cell testing configuration and in the permeation measurements performed here. The requirements for porosity in the cathode would therefore be even more stringent compared to the case of button cell tests with a perpendicular flow of reactant gases to the electrodes, so the inclusion of sufficient cathode porosity would have to be verified in full-cell, high current density tests with bi-polar plate interconnects to ensure that the cathode microstructure is suitable for those operating conditions.

4. Conclusions

Porous composite cathodes containing LSM and YSZ for SOFCs have been successfully fabricated by APS. Screening tests were first used to determine the range of plasma conditions over which LSM and YSZ could be successfully deposited. Using data from these screening tests, conditions were identified which were expected to be suitable for the co-deposition of the two materials for a composite cathode.

The microstructures of LSM/YSZ composite cathodes produced using different combinations of APS parameter values were then examined using a Uniform Design experimental approach, and the conditions that produce the desired microstructures identified. To produce a composite cathode with the desired characteristics requires deposition conditions which allow for both LSM and YSZ to be present in sufficient quantities, and which result in a coating with sufficient porosity such that a high reaction surface area results. The reaction surface area consists of the triple phase boundary regions where LSM, YSZ, and open porosity are in contact with each other and also connected throughout the electrode, so sufficient quantities of each phase are required to obtain a high reaction surface area that results in a low polarization resistance of the cathodes. Coatings produced in moderate energy density plasmas at short standoff distances best satisfy these requirements.

Electrochemical testing of four APS LSM/YSZ cathodes produced using different deposition conditions revealed significant differences in performance. It was expected that cathodes having more porous microstructures would perform better than those with lower porosity, containing dense, extensively melted material. While the best performance was indeed obtained from a coating with a more porous microstructure than the average coatings produced, it was found that other factors, notably low absolute deposition efficiency, can result in inferior performance from coatings with otherwise very desirable microstructures. Both good microstructures and the ability to deposit well-adhered layers in a reasonable amount of time are necessary qualities for APS SOFC cathodes. By utilizing conditions that allow both reasonable porosity and good deposition efficiency, LSM/YSZ composite cathodes with very low polarization resistances have been successfully fabricated by APS, thus offering the potential, when combined with suitable plasma sprayed electrolyte and anode layers, to mass produce SOFCs at greatly reduced processing time and cost compared to conventional manufacturing techniques.

Acknowledgements

The authors gratefully acknowledge the generous support of Northwest Mettech Corp. and the Natural Sciences and Engineering Research Council of Canada and the assistance of Mr. Dave Waldbillig with scanning electron microscopy and of Dr. Michael Poon with design of the helium permeation tester.

References

[1] N.Q. Minh, T. Takahashi, Science and Technology of Ceramic Fuel Cells, Elsevier, Amsterdam, 1995, pp. 1–14.
[2] D. Stöver, H. Buchkremer, S. Uhlenbruck, Ceram. Int. 30 (2004) 1107–1113.
[3] S.P. Jiang, J. Power Sources 124 (2003) 390–402.
[4] P. Charpentier, P. Fragnaud, D.M. Schleich, E. Gehain, Solid State Ionics 135 (2000) 373–380.
[5] K. Huang, P.Y. Hou, J.B. Goodenough, Solid State Ionics 129 (2000) 237–250.
[6] M. Žadyvdas, S. Tamulevičius, T. Grinys, Mater. Sci. (Medžiagotyra) 10 (2004) 349–352.
[7] M. Lang, T. Franco, G. Schiller, N. Wagner, J. Appl. Electrochem. 32 (2002) 871–874.
[8] J. Fleig, Annu. Rev. Mater. Res. 33 (2003) 361–382.
[9] E.P. Murray, M.J. Sever, S.A. Barnett, Solid State Ionics 148 (2002) 27–34.
[10] S. de Souza, S.J. Visco, L.C. De Jonghe, Solid State Ionics 98 (1997) 57–61.
[11] L. Rose, O. Kesler, Z. Tang, A. Burgess, J. Power Sources 167 (2007) 340–348.
[12] M.J.L. Ostergard, C. Clausen, C. Bagger, M. Mogensen, Electrochim. Acta 40 (1995) 1971–1981.
[13] T. Tsai, S.A. Barnett, Solid State Ionics 93 (1997) 207–217.
[14] J. Deseure, Y. Bultel, L. Dessemond, E. Siebert, Electrochim. Acta 50 (2005) 2037–2046.
[15] G. Schiller, R. Henne, M. Lang, M. Muller, Mater. Sci. Forum 426–432 (2003) 2539–2544.
[16] O. Kesler, Mater. Sci. Forum 539–543 (2007) 1385–1390.
[17] R. Hui, Z. Wang, O. Kesler, L. Rose, J. Jankovic, S. Yick, R. Maric, D. Ghosh, J. Power Sources 170 (2) (2007) 308–323.
[18] K. Barthel, S. Rambert, Thermal spraying and performance of graded composite cathodes as SOFC-component, in: W.A. Kaysser (Ed.), Proceedings of the 5th International Symposium on Functionally Graded Materials, Dresden, Germany, October 26–29, 1998, Trans Tech Publications Ltd., 1998, pp. 800–805.
[19] A. Kucuk, R.S. Lima, C.B. Berndt, J. Am. Ceram. Soc. 84 (2001) 685–692.
[20] K. Barthel, S. Rambert, Processing and electrochemical behaviour of LSM–YSZ composite cathodes by vacuum plasma spraying, in: P. Stevens (Ed.), Proceedings of the 3rd European Solid Oxide Fuel Cells Forum, 1998, Nantes, France, European Fuel Cell Forum, 1998, pp. 11–18.
[21] R. Zheng, X.M. Zhou, S.R. Wang, T.-L. Wen, C.X. Ding, J. Power Sources 140 (2005) 217–225.